

G. Schön
U. Simon

A fascinating new field in colloid science: small ligand-stabilized metal clusters and possible application in microelectronics

Part I: State of the art

Received: 7 July 1994
Accepted: 10 August 1994

Abstract Small metal clusters, like $\text{Au}_{55}(\text{PPh}_3)_{12}\text{Cl}_6$, which fall in the size regime of 1–2 nm are colloidal nanoparticles with quantum properties in the transitional range between metals and semiconductors. These chemically tailored quantum dots show regarding the Quantum Size Effect (QSE) a level splitting between 20 and 100 meV, increasing from small particle sizes to the molecular state. The organic ligand shell surrounding the cluster acts like a dielectric “spacer” generating capacitances between neighboring clusters down to 10^{-18} F. Therefore, charging effects superposed by level spacing effects can be observed. The ligand-stabilized colloidal quantum dots in condensed state can be described as a novel kind of artificial solid with extremely narrow mini or hopping bands depending on the chemically adjustable thickness of the ligand shell and its properties. Since its discovery, the Single Electron

Tunneling (SET) effect has been recognized to be the fundamental concept for ultimate miniaturization in microelectronics. The controlled transport of charge carriers in arrangements of ligand-stabilized clusters has been observed already at room temperature through Impedance Spectroscopy (IS) and Scanning Tunneling Spectroscopy (STS). This reveals future directions with new concepts for the realization of simple devices for Single Electron Logic (SEL).

Part I presents the fundamental aspects of small ligand-stabilized metal clusters as well as their physical properties, emphasizing their electronic and optical properties with respect to dielectric response at ambient temperatures.

Key words Ligand-stabilized metal clusters – nanoparticles – quantum dots – single electron logic – microelectronic devices

Prof. Dr. G. Schön (✉) · U. Simon
Institut für Anorganische Chemie
Universität Essen
Schützenbahn 70
45127 Essen, FRG

Colloid-chemical aspects

In most textbooks on “colloid chemistry,” one can find that Ostwalds Welt der vernachlässigten Dimensionen [1] deals with “two-phase systems” where one phase (the dispersing agent) is dispersed with a peculiar degree of distribution in a second phase (the dispersion medium) [2]. Only secondarily are rather approximate data on the size

of colloids given, e.g., for dispersion colloids with a number between 10^3 and 10^9 particles and for association colloids starting with a size of approximately 1 nm. The size and shape of the colloidal particles generally play a subordinate role.

Up to now, only a few special publications [3] have indicated that small nano-sized semiconductor particles represent so-called Q-particles. This term is used to describe quantized matter revealing a wide range of

transitions from colloid to molecule quantum mechanical effects: The so-called *Quantum Size Effect (OSE)* expresses itself in a “blue-shift” of the light absorption which is directly related to the size-dependent change of the corresponding band gap [4–6]. The underlying consideration as Q-particles, i.e. “quantum dots” or “quantum wells,” is based on the conceptualization of electrons as “particles in a box” which is well known from quantum mechanics.

Referring to Ostwalds two-phase colloidal systems, it is often neglected that colloids in the nano-regime can exist without a dispersion medium. In many cases the particles can be recovered from the colloidal solution by carefully removing the solvent. Then, stable powders are obtained which can be subsequently redissolved to yield the original colloidal solutions. This is particularly true for many ligand-stabilized *metal clusters*. The first and most famous with 55 gold atoms was discovered by Günter Schmid in 1981 [7]. Such transition metal clusters are synthesized following absolutely classical colloid-chemical methods of preparation and precipitation in combination with metal-organic techniques. In these cluster types, the organic ligand shell takes over the task of protection, and prevents the single metal cores from coalescence to bulk material. Since, at most, such cluster research has only been performed in the past 10 years, this class of materials has not yet found an entry into colloid science. This is surprising because Ostwald had already in fact reserved a place for them, and because these metal clusters have the invaluable advantage that they can be prepared on mol-scale as particles with uniform size and shape – even with an equal number of atoms per particle with a defined structure. As an example, Fig. 1a shows an Au_{55} cuboctahedron without the ligand shell and Fig. 1b the ligand coordination of $\text{Au}_{55}(\text{PPh}_3)_{12}\text{Cl}_6$, named in the following as “normal” Au_{55} . The large circles represent the “umbrella” shape of the PPh_3 ligands.

The spherical habitus of the “normal” Au_{55} clusters, each cluster having a diameter of 2.1 nm is demonstrated in a *Scanning Tunnel Microscope (STM)* image (Fig. 2) [8].

In recent years, much progress in cluster chemistry has been made with the use of novel – mostly solid-dispersion media. Besides embedding clusters in glasses or polymers [9], the inclusion of clusters of varying sizes in zeolites as dispersion medium [10,11] (possibly as ordered superlattices) has been successful. In this case, the dispersion medium is named “host-lattice” or “solid matrix.” Also recently, the occupation of AlPOs with the Buckminsterfullerene C_{60} was successful [12].

The condensation or crystallization of ligand-stabilized clusters represents an entirely new possibility to build novel materials. Because of the uniform size and exceptional stability of the ligand-stabilized clusters, the colloidal Q-particles as building units can act like atoms in normal

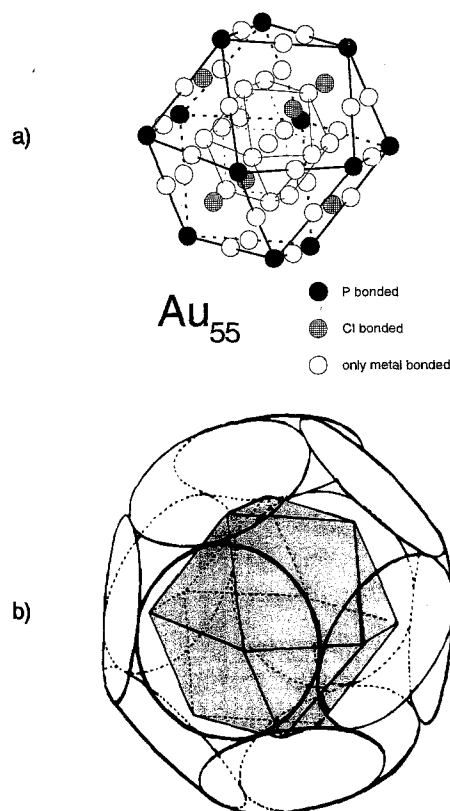


Fig. 1a–b a) The assumed Au_{55} cuboctahedron without ligand shell. b) Ligand coordination of $\text{Au}_{55}(\text{PPh}_3)_{12}\text{Cl}_6$, labeled as the “normal” Au_{55} . The large circles represent the “umbrella” shape of the PPh_3 ligands

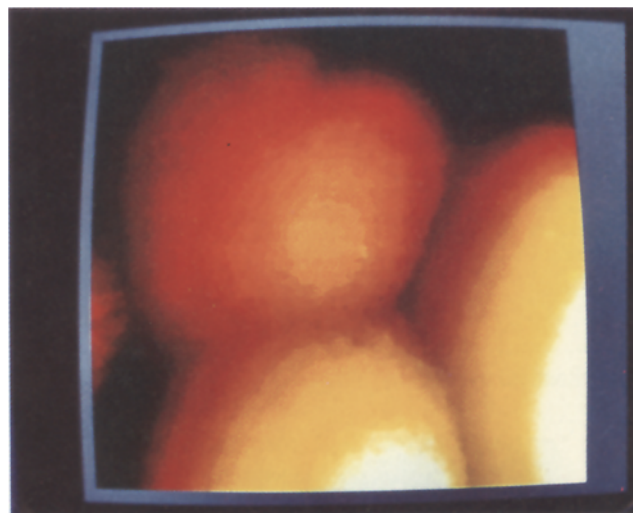


Fig. 2 Scanning Tunnel Microscope (STM) picture illustrating the spherical habitus of individual “normal” Au_{55} clusters with a diameter of 2.1 nm

molecules, compounds, and solids to give novel solids with well-defined dimensions and packing. In these materials the clusters will partially preserve their identity and individuality as quantum dots, but further, should yield as a result of their bonding into the community *novel collective properties* – among others, new electronic and optical features. As with bonded atoms, it will then depend on the method of investigation whether the clusters will show the properties of the individual or those of the collective.

Therefore, the present paper mainly deals with the electronic and optical properties of Q-particles from ligand-stabilized metal clusters and their collective properties with the intention to give information about possible future applications of these or similar building elements. Specifically, *part I* includes the state of the art, and *part II* deals with more speculative future directions. Such unusual materials hold-even at room temperature-many *sophisticated chances for application*, e.g., in digital electronic circuits with single electrons: In *Single Electron Logic (SEL)* [13] as *Single-Electron-Tunneling (SET)-transistor* [14, 15], as *switches in the nanometer-range* [16, 17] or in *high-sensitive electrometers, current-standards, fast oscillators* [14]. Besides *quantum lasers* [16] and *photo cells* [18], components for the *nonlinear optics and optoelectronic switches* [16] operating simultaneously with photons and electrons could be realized. Such components could enable the development of new generations of computers with extremely high capacities.

The exploration of QSE in quantum dots and their collective interaction in novel solids is a challenge for chemists, physicists, and material scientists, but is also of basic importance for the study of theoretical problems in quantum physics.

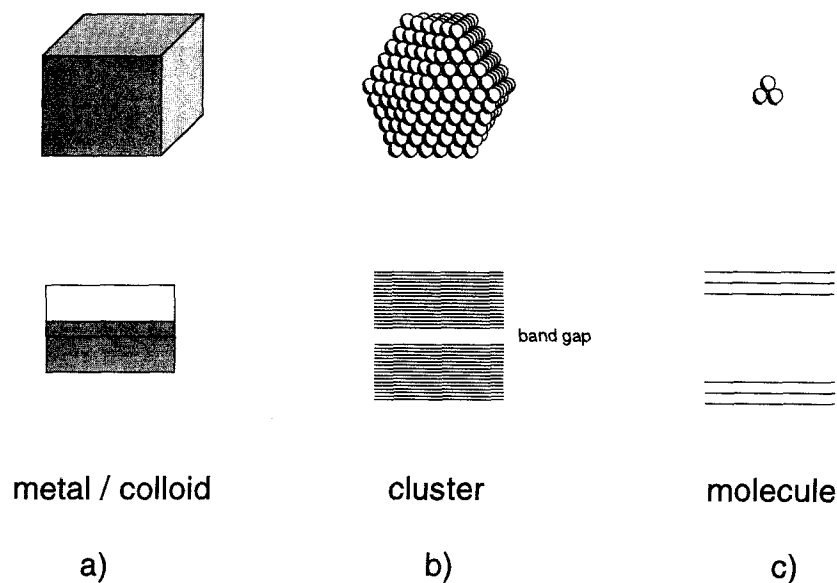
Quantum Size Effect (QSE) in small metal-particles

The availability of small solids like transition metal clusters [20] offers a field of research that raises basic questions: How small a number of atoms is necessary until the properties of the original metal are lost? How does an ordered accumulation of atoms behave? When it is no longer under the influence of its ambient bulk matter? And perhaps most important for “nanoscientists”: What are the future directions for nanotechniques and the applications of the new materials, e.g., in microelectronic devices?

An increasing number of scientific groups is engaged in achieving the latter goal. However, until recently – besides more exotic applications such as reflecting surfaces-chemists had been mainly interested in their potential in heterogeneous catalysis. This field of application for colloids and stable metal-clusters will not be treated in this paper. However, we would like to point out that for this use, in the range between metal and molecule, size and shape play a more important role than the problem of uniform size distribution.

If a metal particle, initially having bulk properties, is reduced in size to a few hundred or dozens of atoms, the density of states in the valence and conductivity bands decreases to such an extent (Fig. 3a–c) that the electronic properties change dramatically, i.e., conductivity, magnetism, etc. begin to disappear. The quasi-continuous density of states is replaced by a discrete energy level structure, with a level spacing, for example, larger than the characteristic thermal energy $k_B T$ (Fig. 3b). The situation in molecular clusters is simple. Three metal atoms, for instance, form energetically well-defined bonding and antibonding mo-

Fig. 3a–c Illustration of the electronic states in a) a bulk metal with typical band structure, b) a larger close-packed cluster already with a small band gap, and c) a triatomic cluster with bonding and antibonding molecular orbitals



molecular orbitals (Fig. 3c). With respect to the size-dependent decreasing electrical conductivity, in 1986, Nimitz et al. [21,22] addressed the so-called *Size Induced Metal-Insulator Transition (SIMIT)*. This refers to a transition due to a geometrical limitation of extended states with a corresponding De Broglie wave-length when the volume of metallic particles is strongly reduced by fractionation, beginning with a diameter of 1 μm , down to an experimental limit of below 20 nm. This effect was detected by measuring the microwave absorption of small particles of solid or liquid indium metal dispersed in oil. Its explanation claims that the boundaries of these particles are potential walls where the electrons are localized inbetween, and that the conduction electrons form standing electron waves with multiples of half of the De Broglie wavelength $\lambda/2$, thus leading to the picture of “particles in a box.” But the corresponding level spacings of these electron states in the above size regime are still smaller than the characteristic thermal energy, so that the temperature dependence of the conductivity of these particles is only slightly affected. This means that the particles are still metallic. The first attempts to take advantage of this effect was the design of so-called *Cut Off Wavelength- (COW-) transistors* [23].

This “size-quantization” effect may be the onset of the metal – semiconductor transition at the very end of metallic behavior of much smaller particles. The size at which the transition occurs depends on the type of metal and the criterion chosen for metallicity as well as the method of investigation. Keeping this in mind, the term “SIMIT” should not be fixed to the change in the electrical conductivity, but be generalized by means of additional indicators. Indeed, the results of a number of recent physical investigations on ligand-stabilized transition metal clusters, reported mainly in sections 5 and 6, lead to the conclusion that coming from the molecular state, metal particles with about 50–100 metal atoms and a diameter between 1–2 nm just barely show metallic behavior [24]. This conclusion also follows from the prediction of the level spectrum of a Au_{55} cluster by a first principle calculation [25].

Why are these metallic Q-particles expected to reveal new electronic properties as soon as the boundary conditions given by its dimensions (e.g., its diameter) reach the order of magnitude of the De Broglie wavelength of the “valency” electrons? The answer is given by quantum mechanics with Heisenberg’s uncertainty principle. Position and momentum of an electron cannot be destined with the same accuracy. The more one electron is spatially confined, the broader its range of momentum. Hence, its medium energy will no longer be determined by its chemical origin but only by the dimension. Electrons localized as “particles in a box” within zero-dimensional quantum dots lose their freedom in all three dimensions leading to discrete energy states, as long as their energy is not high

enough to break out of this confinement. Whenever it is in the magnitude of the electron wavelength $\lambda/2$ or even smaller, quantum effects govern the wave propagation of the system. This effect is called the *Quantum Size Effect (QSE)*. So, by nature, metal clusters of the above diameter seem to be *chemically size-tailored quantum dots* in which some few electrons can be localized, both in terms of geometry and quantum mechanics.

To distinguish the common features of the above described colloidal quantum dots, and to separate them from semiconductor materials, one should note the following: Principally, semiconductors have already in the macroscopic bulk state a band gap. The size-dependent change in mesoscopic particles by the QSE can be observed simply and precisely by optical absorption spectroscopy [6]. On the other hand, a dot made from a metallic particle has many more conductance electrons than a dot from semiconductor material of the same size and yet not a band gap. For this, the dot should actually be much smaller. For instance, the wavelengths of metallic electrons can reach up to 0.5 nm (in comparison, the wavelength in semiconductors, because of the effective mass can be as long as 1 μm). In contrast, based on the Fermi energy of bulk gold, the wavelength of the valency electrons at the Fermi level for Au_{55} (Fig. 1) with $\lambda/2$ would be ≈ 0.1 nm. This wavelength is too small for a particle between 1–2 nm. So far the influence of size quantization with metal clusters seems to be much smaller than with mesoscopic semiconductor particles and possibly undetectable since the metal dot would have to be reduced to such a small size that it would be only a small *molecular* object. On the other hand, according to SIMIT the metal dot will turn out to be a “semiconductor.” Consequently, it seems likely to postulate the existence of formerly metallic “valency” electrons with an effective mass for it. Assuming one of 10%, there could be reached the above cited boundary condition. *Within dots of the same small size built of semiconductor materials this “size effect” would have already taken place, converting them to insulators.*

The latter more speculative considerations are less important, since now the small metal clusters can, for certain, be called “quantum dots,” they being mesoscopic confinements characterized by a set of discrete energy levels according to the predictions for a possible level splitting in Au_{55} [17, 24–27]: The not yet completely evaluated *Scanning-Tunnel-Spectra (STS)* of “normal” Au_{55} , which was actually examined at room temperature [28], reveal fine structures with oscillation intervals of about 100 mV (see Fig. 11, section 2.3, part II). Furthermore, it was recently found and fitted at 4.2 K with the same method that even the larger Pt_{309} metal cluster reveals a level splitting of 20 meV by an additional structure in the Coulomb staircase [29]. This spacing is more

pronounced than expected based on the formula of Halperin [30] (see Fig. 9, section 6). However, since the outer shell of the four-shell Pt-cluster is not typically metallic (like in any ligand-stabilized metal cluster, the electrons of the outer shell bond more strongly, see section 5), only the diameter of the inner metallic core (~ 1.6 nm) consisting of only 147 Pt-atoms arranged in three shells should be taken into consideration. This value comes much closer to the experimental value. Furthermore, the high symmetry of the cluster might cause some degeneration leading to a larger level splitting [31].

The Single-Electron-Tunneling Effect (SET) in Single Electronics (SE)

Since 1985, when Licharew and Zorin [32, 33] theoretically predicted how to manipulate individual charge carriers, *Single Electronics (SE)* as a separate direction in its own was born. Soon after, the discrete transfer of single electrons was experimentally verified in ultrasmall metal-insulator-metal sandwich structures (with 1 nm interlayer distances) called tunnel junctions [34]. It was demonstrated that the discreteness of the electric charge e becomes essential and a quantum mechanical tunneling of electrons through such junctions can be effected by

Coulomb interaction, controlled by an external voltage or charge injection. This effect, named *Single Electron Tunneling (SET)* is today accepted to be *the future concept for the ultimate miniaturization in microelectronics* [15].

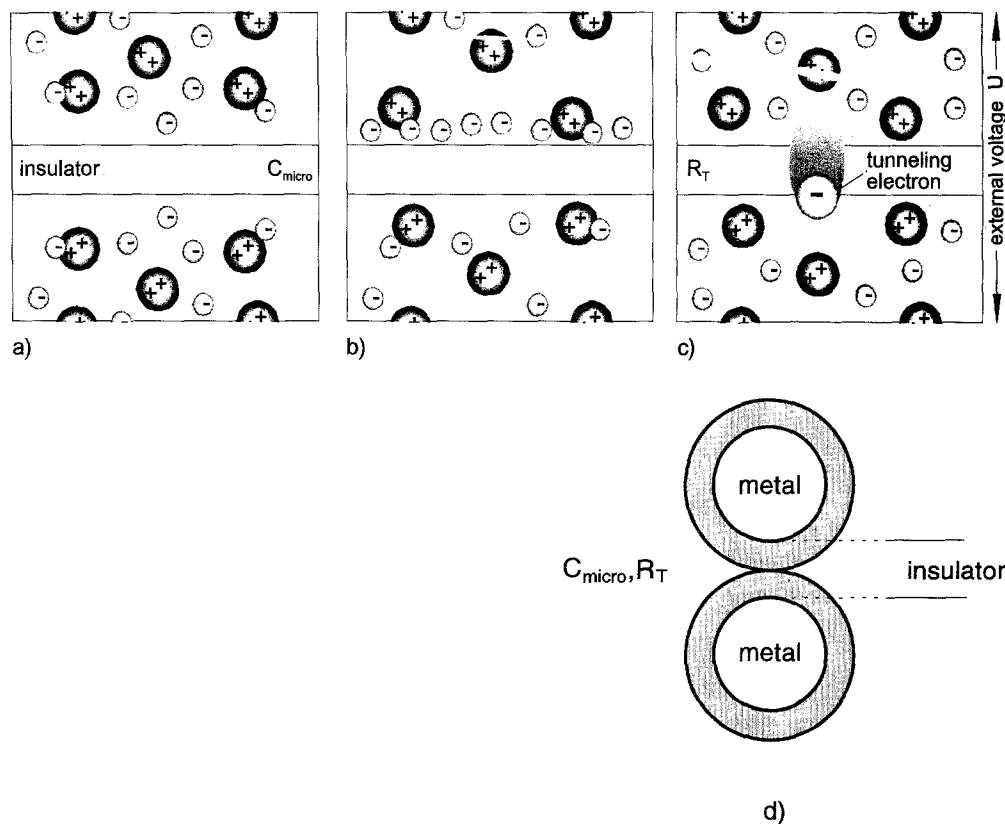
Considering an isolated piece of metal, its number of electrons is always integer. The controlled transfer of single electrons between two metal islands can only be realized when *two principal conditions* are fulfilled:

- The insulating energy barrier must be rather opaque for charge carriers. This condition can be formulated by the transition or tunnel resistance R_T of the junction. With $R_T \gg R_Q$ the barrier should be much higher than the von Klitzing resistance quantum $R_Q = h/e^2 = 25.8$ k Ω . In this state the electrons in the metal islands can be considered as localized and the SET can be understood by classical physics.

- In order to make the exchange of electrons controllable, the Coulomb energy E_c associated with charging by *one* extra electron with $e^2/2C_{\text{micro}} \gg k_B T$ must be much higher than the thermal energy, whereby the parameter C_{micro} is the total island capacitance.

When the above conditions are satisfied, the system can be switched on by starting with a definitive external voltage U by means of single charge carriers tunneling: Then, individual electrons drip from one metal island to the other (Fig. 4a–c) similar to a dripping water faucet.

Fig. 4a–d The tunneling of a single electron between two metal particles through a small insulating junction. a) At the beginning the boundary is uncharged, then b) by external voltage U the charge carriers are gathering at the tunnel junction, and c) finally, one single charge “drips” through the insulating layer. d) The corresponding situation with a pair of small ligand-stabilized clusters in contact. The metal islands now have the dimension of quantum dots



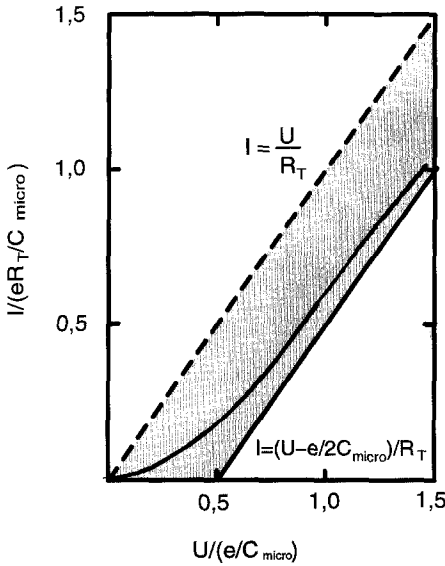


Fig. 5 I-U-characteristics for Single Electron Tunneling (SET). The dotted line would be Ohmic behavior. The shaded region is the domain of the Coulomb blockade with one non-linear characteristics typically shifted by $e/2C_{\text{micro}}$

In a rough simplification, current-voltage characteristics (I - U -curves) resemble those in Fig. 5 [14]. With Ohmic behavior the expected curve would be the dotted straight line; however, when single electrons are tunneling at temperatures $T > 0$ K the curves are nonlinear, lying only within the shaded region limited asymptotically by a parallel line. The latter is characteristic at $T = 0$ K, with an offset of voltage averaged in time $|U| = 0.5e/C_{\text{micro}}$ named *Coulomb blockade*.

Due to the fact that a rise of the bias voltage increases the number of channels for tunneling of single charge carriers, a series of Coulomb blockades often occur, resulting in a step-like structure in the current-voltage characteristic which is called *Coulomb "staircase"*.

The characteristic times τ_{micro} of such transitions range from about 10^{-11} s (e.g., for $R_T = 100$ k Ω and $C_{\text{micro}} = 10^{-16}$ F) up to several hours according to $\tau_{\text{micro}} = R_T C_{\text{micro}}$.

Furthermore, there exists a fundamental relationship for correlated tunneling through a SET-junction:

$$v_{\text{SET}} = I/e. \quad (2)$$

With a constant current I , charge and voltage are oscillating with the so-called SET-frequency v_{SET} .

The idea of SET and its simple principles were somewhat surprising for our progressive era in which immense research expenditure is customary. Besides, the dealing with single electrons was not completely new, but had only sunk into oblivion: Already in 1909, Millikan succeeded in

finding the elementary charge e of a single electron with his famous oil-droplet experiment [35]. Furthermore, mankind has made use of the tunnel effect since the invention of electrical switches in which on the nanometer scale the metal contacts never actually touch, i.e., electrons must bridge the last nanometer by tunneling. As for the QSE and the pieces of matter which today are named "quantum dots," already in 1938, Fuchs pointed out that electrons, if enclosed in small structures of some few nanometers should show extraordinary quantum mechanical properties [36].

In order to satisfy the above-mentioned conditions for lithographically made circuits, samples must be, presently, cooled down to the millikelvin range. This toilsome work is necessary because the capacitances C_{micro} are still too high, even when scaling down to 0.1 micrometer. Applying the SET effect with quantum dots for an ultimate miniaturization means in practice to reduce matter to a colloidal or molecular size with a number of atoms somewhere between 10 and 1000 and, moreover, to contact it for addressing [37]. One intention of the present paper is to show that it is quite possible to reach this goal with chemically size-tailored, ligand-stabilized, metal quantum dots. Additionally, these dots offer the invaluable advantage that they allow the application of the SET effect even at room temperature.

However, the utilization of small clusters with quantum dot dimensions (Fig. 4d) as metal islands complicates the physics of SET because the clusters are only one order of magnitude larger than their constituting atoms. Due to the QSE (section 2) such a small size of metal clusters changes its energy spectrum to a small potential energy well with a set of distinctly discrete energy levels. Now, the two principal conditions described for the "classical" SET effect require some modification.

First, a tunnel junction can hardly be described by such a simple parameter as a constant tunnel resistance R_T . Strictly, such an approximation is only valid when the densities of levels in both metal islands are high and independent of energy.

Secondly, the macroscopic electrostatic approach fails when a conductor is treated as a continuous body with an infinitely thin screening depth. Moreover, as the number of conductance electrons in the cluster decreases, the electron-electron interaction is not completely screened out. Hence, the concept of electric capacitance does not strictly work anymore. In this case the charging energy should be calculated by directly counting the energy of interacting charges. The Coulomb energy can still be roughly described with the same elementary formula for the charging energy of a capacitor. Then, the symbol C_{micro} already denotes an amount which is generally dependent on the total number of interacting electrons occupying the cluster.

These peculiarities do not mean that charging effects in small clusters are eliminated. Theory shows [19] that the basic result of SET still remains, and new features develop. For example, the current-voltage characteristics of a double junction with a quantum dot will have, besides the Coulomb staircase, a fine structure due to the energy quantization inside the dot. Then, not only steps in the current by incremental charging of the cluster will be present, but also extra steps from the QSE. These additional steps result whenever the bias voltage reaches a value so that the next discrete level of the quantum dot can contribute. This effect has been recently experimentally verified for metal clusters [29] (cf. section 2, this work and section 2.3, part II). Hence, the single electron charging effect and the QSE do not contradict one another but, in fact, coexist. We will call this situation *Energy Quantized Single Electron Tunneling (QSET)*.

State of the art: preparation and general view of stabilized metal clusters

In the following, we give a brief overview of the different types and preparation techniques of stabilized metal clusters and colloids. In addition, several methods are known for the synthesis of naked or bare metal clusters, i.e., molecular beam techniques [38] or matrix techniques [39]. Although the bare, non-protected clusters are also excellent objects to study the evolution of metallicity, the main difficulty is their very short life time and their high reactivity. Furthermore, cluster samples prepared by these techniques reveal a more or less broad size distribution, a problem which has not been solved. Since there exist several reviews [40] detailing the techniques, possibilities and frontiers on the field of bare clusters, we exclude them from our consideration. Instead, the focus here will be on stabilized metal clusters and colloids. Since the problem of size distribution has partially been solved, these ligand-stabilized clusters are for the first time ideal objects to study the properties of uniform particles.

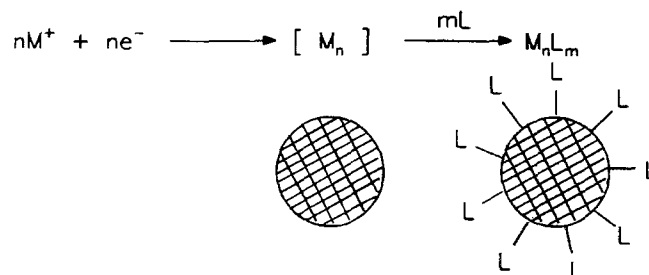
Ligand-stabilized transition metal clusters

Large ligand-stabilized transition metal clusters can be synthesized by dissolving in a suitable solvent metal ions of salts or complexes and reducing the metal to an oxidation state 0. This procedure is well known in colloid chemistry and is usually applied to prepare precipitates of gold or silver on glass. To prevent the formation of larger macroscopic metal particles, the growth of the metal aggregates must be controlled. This is successfully effected by adding nitrogen or phosphorus-based ligands as electron

pair donors to saturate the free valences on the surface of a growing particle.

The size of a cluster is determined by the so-called geometric magic numbers of metal atoms. These numbers result from a closed geometry of the densest sphere packing of metal atoms. For example, in one such arrangement a central atom is surrounded by 12 nearest neighbors forming a closed shell ($1 + 12 = 13$). Furthermore, this 13-membered aggregate can be surrounded by a second shell of 42 atoms to form a completed structure of 55 atoms ($13 + 42 = 55$) and so on. In each new shell n , $10n^2 + 2$ atoms can be incorporated into the aggregate. Electronic magic numbers are also known [41] which describe the stability the metal cluster (especially of bare clusters) in terms of electronic shell structures and similar to atom nucleus models. Using the model of the geometric magic numbers, the size and stability of most clusters synthesized to date can be understood.

The strategy of preparation is illustrated in the following simplified scheme:



Using this route, clusters of varying sizes have been synthesized as listed in Table 1.

Figure 6 illustrates the arrangement of metal atoms in full shell clusters assuming a cuboctahedral symmetry. The transition metals used for cluster synthesis are usually noble metals like Pd, Pt or Au, which have a pronounced tendency to form larger metal complexes [42]. Suitable ligands include especially phosphine and phenanthroline or related compounds.

The most preferred method of characterization of metal clusters is *High Resolution Transmission Electron*

Table 1 The ligand-stabilized transition metal cluster sizes with geometric magic numbers synthesized up to now

Cluster	M ₅₅	M ₃₀₉	M ₅₆₁	M ₁₄₁₅	M ₂₀₅₇	Colloid
Number of shells	2	4	6	7	8	> 10
Metal	Au, Pt, Rh	Pt	Pd	Pd	Pd	Au, Pd, Au/Pd, Au/Pt, Pt/Pd

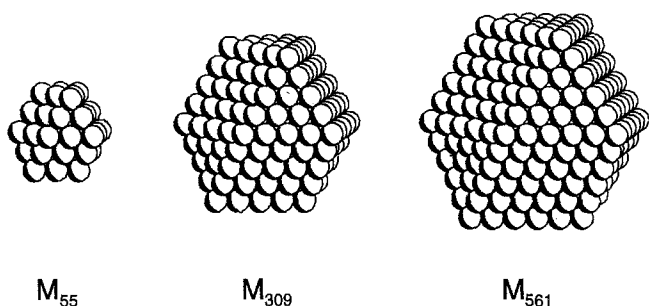


Fig. 6 Examples for the arrangement of metal atoms in the full shell clusters M_{55} , M_{309} and M_{561} . The ligand shells are omitted

Microscopy (HRTEM). Figure 7a–c show some micrographs of the above-mentioned clusters in atomic resolution (see also [42]).

Clusters and colloids of this type have only a weak tendency to crystallize. Therefore, only amorphous or microcrystalline powders are isolated after removing the solvent. The solid itself is stable under ambient conditions and can be redissolved in a suitable solvent.

Besides monometallic colloids, larger mixed metal colloids are known, such as Au/Pd, Au/Pt, and Pt/Pd. Here, their catalytic properties are of major interest [43].

Apart from pure transition metal clusters, there also exist metal clusters containing fifth or sixth main group elements. Stabilizing ligands are also phosphanes, PR. Examples range from small chalcogenide clusters like $\text{Cu}_{20}\text{Se}_{13}(\text{PR}_3)_{12}$ up to 146 Cu-atoms [42]. In the high nuclear clusters, like $\text{Cu}_{70}\text{Se}_{35}(\text{PR}_3)_{22}$ (Fig. 8), the structural principle of the bulk Cu_2Se dominates, in other words Cu^{1+} ions occupy vacancies between penetrating Se-layer structures.

The “diameter” of the Cu_2Se -core in the Cu_{70} -cluster is approximately 2.5 nm (“height” of the triangle). In comparison, with 1.4 nm the metal core of the pure metal cluster Au_{55} is distinctly smaller. Of particular interest for

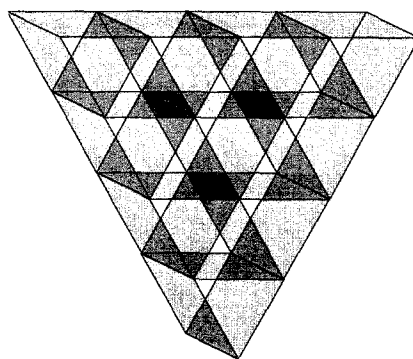


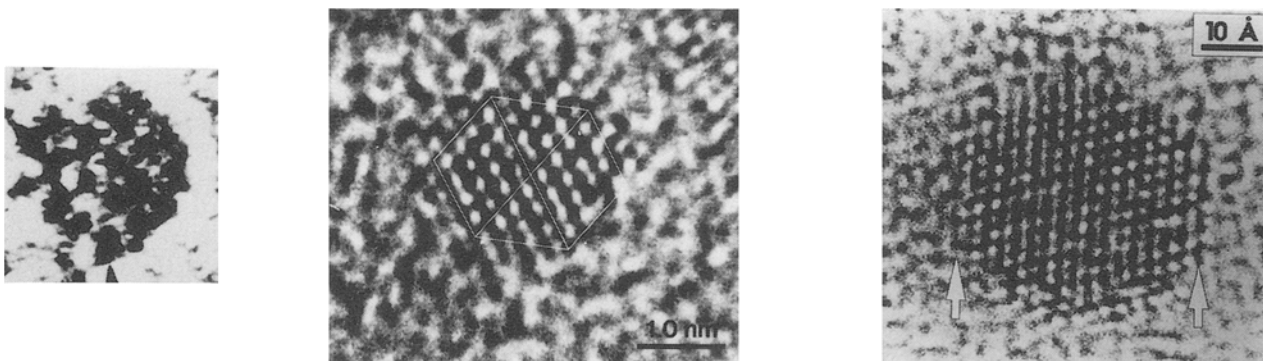
Fig. 8 Geometry of the $\text{Cu}_{70}\text{Se}_{35}(\text{PEt}_3)_{22}$ core (without ligand shell) indicating the crossing CuSe_2 bands. This cluster compound illustrates the possibilities for the chemically size-tailoring of non-spherical quantum dots

further developments is that, with the Cu-Se cluster: quantum dots with non-spherical shape can be generated (c.f. section 1, part II). Furthermore – in contrast to the pure metal clusters – these semiconductor clusters can be crystallized easily to solids upon removing the solvent. Here, the Cu_2Se -particles are ordered, following the principles of densest package. However, quite disadvantageous for possible applications is the fact that these cluster compounds are only stable under protective atmosphere.

Metal clusters in inorganic host lattices

Instead of stabilization via organic ligands, metal as well as semiconductor clusters can be stabilized in inorganic hosts. These may be porous amorphous polymers or glasses as well as crystalline zeolites or related molecular sieve type materials [10]. Among these different materials, well-defined crystalline structures are ideal hosts due to their geometrically defined one-, two- or three dimensional pore and/or channel systems, which allow the uniform inclusion

Fig. 7a–c Electron transmission micrographs of a) Pt_{55} , b) Pt_{309} and c) Pd_{2057}



of 0.6 nm up to 10 nm diameter guests [44]. The insertion of large 10 nm clusters is achieved only by local degradation of the host lattice. The synthesis and stabilization of ligand-free metal clusters inside the zeolite can be realized using various routes described in detail in refs. [10, 45]. Some techniques for such cluster preparation consist of thermal decomposition of metal organic complexes [46, 47], reduction of exchangeable metal ions or complexes with reducing agents like hydrogen or alkali metal vapor [11, 48] or zeolite doping directly by alkali metal vapor [49, 50] (see also “black sodalite” in section 6.2).

The major importance of such guest/crystalline host compounds with respect to the application in microelectronics results from the possibility to organize within the three-dimensional host lattice, well-defined cluster arrangements having identical sizes and identical interparticle distances. Such purposeful cluster organization is not possible in glassy or polymer hosts. The cluster structure within the host lattice yields an “inverse lattice” or “superlattice.” Such superlattices are believed to be realized with CdS-clusters [51] in zeolite Y, and with Ag-clusters in sodalite [52].

Future directions of zeolite science in this application field are determined by their high potential to be used in nanoscale optoelectronic devices. Either their well-known molecular sieve properties are utilized like in chemoselective sensors or the properties of the confined guest compound are of major interest for multiple quantum dot devices or nonlinear optical switches.

A review of the properties known to date as well as of some possible applications is given in ref. [10].

Physical properties of ligand-stabilized metal-clusters

The aim of physical investigations on cluster compounds is mainly to determine the “metallic properties” of these materials. “Metallic properties” covers a large field focusing on metallic binding properties, delocalized electrons or collective electron phenomena, magnetic properties, or even metallic structures. With respect to the metallic properties of such small particles, one has to take into account that any physical investigation does not only include information about the cluster, but also about the cluster under the “influence” of its ligand shell or matrix. This is obvious when, for instance, a metal atom has an oxidation state one or two because of its direct interaction with a ligand. This of course means that the properties of a ligand-free non-protected, naked cluster must be necessarily different from the properties of a ligand-stabilized cluster. So the total number of metal atoms forming the complete cluster must be distinguished from the number of inner metal atoms having exclusively other metal atoms as

neighbors. This distinction becomes increasing more important with decreasing cluster size.

Depending on the method, measurements on stabilized clusters have been performed directly on powdered samples, dissolved in an adequate solvent like CH_2Cl_2 or water, or embedded in different organic or inorganic matrices. In the following, we give a brief overview of the studies by different microscopic and macroscopic techniques:

The ^{197}Au Mössbauer spectroscopy is a microscopic technique which allows the determination of the nature of individual sites. For example, the results of Mössbauer spectroscopy of the cluster compound $\text{Au}_{55}(\text{PPh}_3)_{12}\text{Cl}_6$ indicate the presence of four different types of Au atoms [53], 13 inner atoms forming the nucleus of the cluster and three different surface sites. The surface sites can be subdivided into 24 uncoordinated surface atoms, 12 atoms coordinated to the PPh_3 -ligands and six atoms coordinated to the chlorine ligands. These results fit very well with the assumed cuboctahedral structure of Au_{55} (Fig. 1a). The chemical shift caused by the 13 inner atoms, is quite close to that of bulk gold, which means that the 13 atoms build a metallic core. This stands in contrast to the ligand-coordinated and non-coordinated surface gold atoms. The pronounced temperature dependence, which is approximately equal for each contribution of the individual sites, indicates an additional contribution due to the motion of the whole cluster [54]. Besides the indication of metallic properties of the inner cluster core, the Mössbauer studies also allow the calculation of the specific heat of Au_{55} at low temperature, including information about the intra-cluster phonon excitations as well as about the motion of the whole cluster [55]. On one hand, the calculations are in excellent agreement with the experimental data of the low temperature specific heat. This means that the Au–Au bonding in Au_{55} is non-directional and therefore probably metallic. However, on the other hand, the measured specific heat of Au_{55} [56–58] did not reveal any linear term as would be expected if typical metallic conductivity would be present. This indicates the lack of an electronic contribution due to mobile, delocalized electrons to the specific heat. In the larger metal cluster compounds Pt_{309} and Pd_{561} a linear term which can be interpreted as an electronic contribution has been detected [59, 60]. But it is only approximately 1/3 of the bulk value.

The interatomic distances in $\text{Au}_{55}(\text{PPh}_3)_{12}\text{Cl}_6$ have been obtained from several EXAFS measurements [61–63]. It was observed that the Au–Au distance is 0.280 nm in a slightly disordered cuboctahedral structure. This distance is smaller than in the bulk metal with 0.288 nm. Thus, the Au_{55} cluster is compressed into a volume about 10% smaller [55]. On the other hand, the observed Au–Au

distance in bare Au_{55} cluster on a non-conducting substrate is slightly larger than in the bulk material [64,65]. The contraction in the ligand-stabilized cluster can be explained as the result of a loss of electrons (12 valence electrons per cluster) to the ligand shell leading to a decrease of the Coulomb repulsion [55].

Another direct way to investigate the “metallicity” of clusters is the measurement of the *Knight shift* of the nuclear magnetic resonance caused by the Pauli-spin susceptibility of the conduction electrons [26]. The presence of the conduction electrons is the criterion for “metallicity” on the way from the molecular to the metallic state or “metallic behavior”. Platinum shows one of the largest Knight shifts among all metals [66]. ^{195}Pt -NMR studies on $\text{Pt}_{309}(\text{phen})_6\text{O}_{30}$ reveal two signals at $B_0/\gamma_0 = 1.10$ and 1.08 kG/MHz [67]. The analysis of the temperature dependence indicates that the high field peak is caused by Pt spins in a metallic environment and the low field peak by the spins of the surface atoms which are coordinated to the ligand molecules [62]. These investigations impressively show the beginning of metallic behavior in the inner core of 147 Pt atoms of this 309 metal atom cluster compound.

Magnetic measurements have also been performed on stabilized metal clusters. The magnetic response in the case of a magnetic metal like Ni in the metal cluster compound $[\text{Ni}_{38}\text{Pt}_6(\text{CO})_{48}\text{H}]^{5-}$ [68] is much smaller ($\sim 9 \mu_B$ per cluster) as expected from the bulk material. Each Ni atom contributes $0.6 \mu_B$. For the Co_{55} cluster, the observed susceptibility value consisting of $\sim 5 \mu_B$ per cluster is also smaller than expected from the bulk; here, each Co atom contributes $1.7 \mu_B$. Similar results have been obtained for various ligand-stabilized M_{55} clusters with non-magnetic metals like Au, Rh, Ru, and Pt. They all show a low susceptibility with a weak increase at low temperatures. Although detailed theoretical calculations of the magnetic properties of these cluster compounds are still lacking, it is clear that the magnetic properties are determined by the bulk properties, the type of ligand, as well as possible absorbates. It can be assumed that the effect of ligand coordination to the surface metal atoms is strongly analogous to the crystal field effect on single metal atoms in simple metal organic complexes [42].

The influence of the ligand shell on the electronic structure of the surface atoms has also been investigated by *SQUID magnetometry* [69]. The results of the measurements on $\text{Pd}_{561}(\text{phen})_{36}\text{O}_{200}$ again confirm the assumption that only the inner core of 309 Pd atoms in this five-shell cluster shows a bulk-like behavior. The remaining surface atoms do not contribute due to the ligation of phenyl groups and oxygen atoms.

Besides these investigations on ligand-stabilized metal clusters, the photoexcitation of naked Au clusters on a supporting substrate reveals an insulator-to-metal

transition at approximately 100 Au-atoms. On the other hand, for Pd clusters such a transition already appears at approximately 25 atoms [70].

Electronic and optical properties of small metal particles and ligand stabilized metal cluster samples

The intention of this section is to present some electronic and optical properties of small stabilized metal clusters with the main focus on possible applications in microelectronic devices and especially in single-electron-tunneling devices (SET-devices) at ambient temperatures. This point of view is very important for microelectronics due to the physical limits of miniaturization; and as discussed in section 2, the use of metal instead of semiconductor materials will have a great advantage with respect to an ultimate miniaturization of such devices.

Size-Induced Metal-Insulator-Transition (SIMIT), as it was introduced in section 2, postulates a certain amount of discreteness of the level structure of the conducting electrons in metallic nanoparticles. Experimental data can be explained by the theory of Kubo [71] and of Gor'kov and Eliashberg [26] assuming an equidistant level spacing Δ . The distance of which can be calculated with the formula:

$$\Delta = 4E_F/3N \sim V^{-1}, \quad (3)$$

where E_F is the Fermi energy of the bulk state and N is the total number of electrons in the particle (depending on the number of valency electrons per atom and on the number of atoms per particle) and V^{-1} is the inverse volume. In 1986, Halperin [30] introduced the Sommerfeld constant of the heat capacitance to improve Kubo's ansatz. With his formula the average level spacing Δ of a small metal particle can be calculated as a function of the particle diameter.

Applying these considerations to the Au_{55} cluster – with the assumption that only the inner core of 13 Au atoms is “metallic” in the above sense – a level spacing of more than 100 meV might be expected (see Fig. 9). This value is in the same order of magnitude as the Coulomb blockade caused by charging of the capacitance between two neighboring clusters constructed by the ligand shell [27]. Therefore, it is not surprising that fine structures of about 100 mV in a not yet completely evaluated STS-experiment are roughly equidistant [28] (see section 2.3, part II).

Independently, first principle calculations also predict a discrete one-electron level spectrum with spacings of about 200 meV up to 700 meV. The spacings are expected to be extremely sensitive to structural deviations from a spherical icosahedral structure [25].

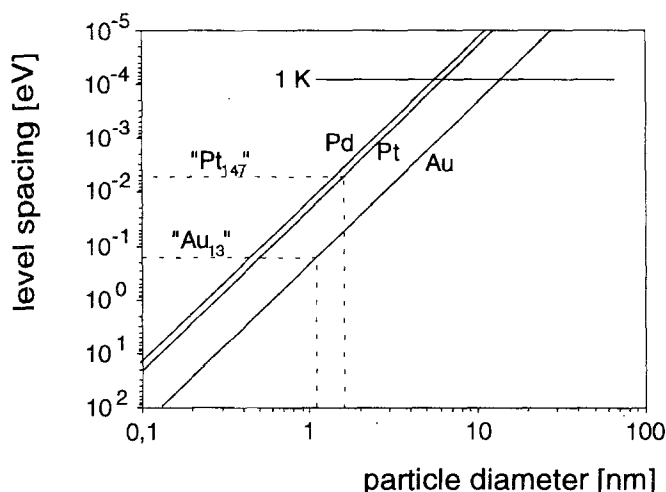


Fig. 9 Average level spacing as a function of particle diameter for some metallic elements according to the formula of Halperin. The level spacing of the inner cores “Pt₁₄₇” and “Au₁₃” can be estimated from this diagram (Fig. according to ref. [30])

Electronic conductivity and dielectric response of ligand-stabilized metal cluster samples

Various DC and AC measurements on ligand-stabilized transition metal clusters have been performed. A review is given in [72]. Measurements on compressed powder samples of Au₅₅(PPh₃)₁₂Cl₆ as well as Pd₅₆₁(Phen)₃₆O₂₀₀ indicate that the temperature dependence of the DC conductivity σ_{DC} follows over a wide range of temperature (70–350 K) the exponential law $\sigma \sim (T/T_0)^{-1/2}$. The frequency dependence of the AC conductivity as well as the nonohmic behavior at strong electric fields discloses a pronounced similarity to different heterogeneous materials, like cermets, doped and amorphous semiconductors or metal- and carbon-insulator composites. This “universal response” [73] was carefully analyzed by different physical models of hopping conductivity with the conclusion that the experimental data can be best fitted with a thermally activated stochastic multiple site hopping process. Unfortunately, these models [72] do not allow any distinction between different local transport mechanisms (tunneling or hopping) or between the chemical nature of the sites (e.g., energy levels in atoms, molecules, clusters, ligand shells, aggregates of clusters or metal particles). Hence, no principal difference was found between different cluster sizes or to the comparative substances.

Our interest was – with respect to the application of single clusters or collectives of “multiple quantum-wells” in SE – to explain or to predict local microscopic behavior.

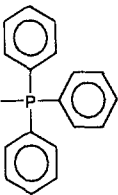
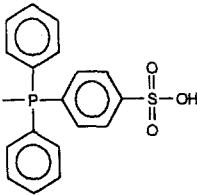
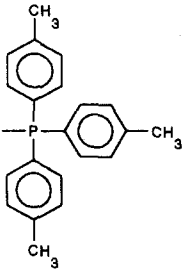
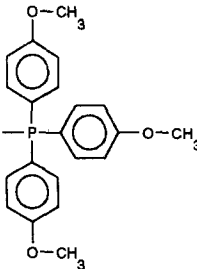
Therefore, *Impedance Spectroscopy* (IS) [27] measurements were performed on four physically and chemically different variants of ligand-stabilized Au₅₅ clusters (c.f. figures in Table 2), the “normal” Au₅₅ (a, see Fig. 1), the water-soluble Au₅₅ (b), the respective with a tolyl-shell (c) and an anisyl-shell (d), and further on the larger Pt₃₀₉ and Pd₅₆₁ clusters. The experiments were conducted in the high temperature range from ambient temperatures up to the respective limit of chemical stability from 253 to 333 K. IS is a powerful characterization method, even for heterogeneous materials, allowing the detection of the effect of alternating, quasi-stationary electrical fields on a sample. The response of the sample is determined by conductance and polarization (capacitive) processes of fixed and mobile charges. Measuring the damping of the amplitude and the phase shift of the resulting current, the frequency dependent complex impedance of a sample is determined, which can be depicted by the real and the imaginary part in the complex plane. This description is only valid in the case of linear behavior which for the cluster compounds is true at low electric fields.

The experimental data collected allow a mathematical description of the response which can be compared with physical models derived from structural information (e.g., in the case of heterogeneous systems Maxwell–Wagner, brick layer, effective medium [74]). The models are typically related to circuit equivalents which allow data fitting characteristic of the system with respect to its properties. Sometimes it is necessary to involve further analytical methods like the deconvolution by inverse Fourier transformation [75], especially when the known physical models fail to describe the system properties.

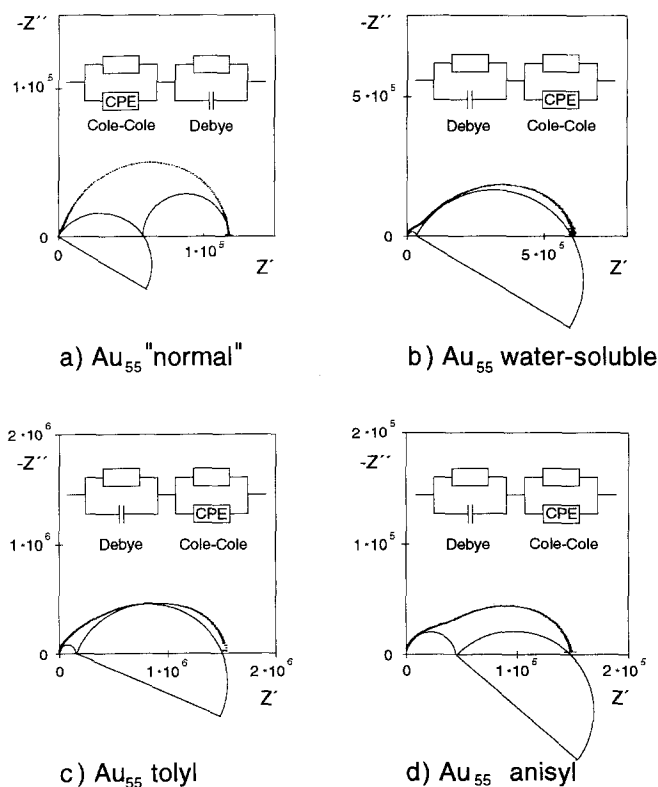
The samples investigated by this method were pressed into disks with controlled high pressure in steps to maximum 1 GPa. Well-prepared disks revealed a gravimetric defined density of more than 90% of the theoretical closest sphere packing (see Table 2). Through re-dissolution in appropriate solvents, chemical and spectroscopic analysis and STM [8] it was verified that the protecting ligand-shells were not destroyed and that the metal cores did not reveal any noticeable aggregation via coalescence.

Impedance measurements on these highly compressed, close-packed samples of ligand-stabilized metal clusters reveal in every case, as a very characteristic feature, two relaxation domains in the kHz or MHz region caused by coupled processes with macroscopic relaxation times [27]. In contrast, samples diluted with unpolar polystyrene did not show either relaxation process. For metal clusters embedded in polar matrices, like for instance zeolites (see section 4.2), relaxations were again observed in the LF region. These relaxations are, however, now caused by coupling with the polar environment of matrix and cations [76].

Table 2 Outline of the four Au₅₅-variants examined, including their formula, ligand type, dimensions, activation enthalpies in the condensed arrangement, and density of packing

compound/ formula name	Au ₅₅ (PPh ₃) ₁₂ Cl ₆ Au ₅₅ „normal”	Au ₅₅ [(PPh ₂ C ₆ H ₄ SO ₃ H)] ₁₂ Cl ₆ Au ₅₅ “water soluble”	Au ₅₅ [P(C ₆ H ₄ CH ₃) ₃] ₁₂ Cl ₆ Au ₅₅ tolyl	Au ₅₅ [P(C ₆ H ₄ OCH ₃) ₃] ₁₂ Cl ₆ Au ₅₅ anisyl
type of ligand				
metal core (nm)	1.4	1.4	1.4	1.4
total (nm)	2.1	2.3	2.2	2.3
E _A Debye (eV)	0.15	0.12	0.23	0.18
E _A Cole–Cole (eV)	0.16	0.15	0.21	0.17
density of the packing (%)*	92	73	66	60

*) Gravimetrically defined density compared to the theoretical closest sphere packing of the spherical cluster molecules

Fig. 10a–d Impedance spectra in the complex plane with calculated fits for compressed discs from the four available variants of Au₅₅ with identical core structure but differing ligand shells. Above are the respective circuit equivalents

The relaxation regions can be resolved by mathematical fitting [77]. Some typical examples of the measurements on Au₅₅ are shown in Fig. 10a–d, where the real part of the impedance is plotted against the imaginary part of the impedance in the complex plane. The total response can be described by the circuit equivalent shown above the experimental curves. Below the measured curves, each separate semicircle is plotted belonging to separate links.

Particularly striking is the fact that one of the two semicircles is always an ideal Debye type. In general, this circle can be visually recognized only in the total non-fitted spectra measured at the highest temperatures. Furthermore, in this high temperature range, the activation enthalpies for the small clusters are very similar, even with different ligand shells (Table 2).

The activation enthalpies were determined from an Arrhenius-behavior $\approx (T/T_0)^{-1}$ such as for the “normal” Au₅₅ with 0.15 respectively 0.16 eV. Here, in this narrow temperature interval an exact distinction from other *T*-dependencies – especially for the Cole–Cole semicircle – cannot be made. Deviation from simply activated behavior should be noticeable only at low temperatures, where the high temperature features are hidden.

The *first process* represented by a distributed Cole–Cole element was interpreted as an “inter”-cluster process (see also [72]) due to the transport of electrons between neighboring clusters.

This was supported by the fact that

- the Cole–Cole element could describe a distribution of relaxation times due to a slight disorder in the arrangement of the clusters, and
- the exponent α of this impedance function at 0.65 is a typical value for hopping conductivity.

On the other hand, the second process with a macroscopic relaxation time of

$$\tau_{\text{Dmacro}} = R_{\text{D}} C_{\text{D}}, \quad (4)$$

represented by the Debye element was interpreted (however not yet with a detailed model like in section 2.2, part II) as an “intra”-cluster process. Assuming in a first approximation, at the capacitance C_{D} that only clusters with ideal cluster arrangements participate, each with the same weight, C_{D} can be divided into contributions of partial capacitances C_{micro} from single clusters (see section 2.3, part II). Assuming that the Debye low frequency relaxations in cluster samples can be explained by *Energy Quantized Single Electron Tunneling* (QSET) like in section 2.4, part II, C_{micro} generally depends on a small total number of interacting electrons occupying the cluster [78], including charging effects. Thus, the distinction between “intra”- and “inter”-cluster processes becomes somewhat marginal. Chemically speaking, this means that two quantum dots form a cluster pair having an interdependent level scheme.

With this premise, the application of a model for cluster–cluster interfaces which successfully defines the energetic density of states at semiconductor–insulator interfaces [79] yields an energetic density of charges per cluster of 10.75 eV^{-1} . This value is also typical for semiconductors. If these charge carriers in spite of the fact that the conductance electrons distribution is no longer purely Fermi and there is electron–electron interaction – are treated like free electrons confined in the quantum box, the Density of States (DOS) is 4.40 eV^{-1} at the Fermi-plane for the smallest quantum box in the ground state with $k_{\text{F}} = \pi/x$, where x is the lateral extension of the box. According to the Pauli principle, it can be occupied by two electrons (Fig. 11) leading to a value of $x = 1.42 \text{ nm}$ which is in good accordance with the real size of the metal core of Au_{55} .

For these, the Fermi energy would be 0.19 eV , and this value is in the same order of magnitude as the measured activation enthalpies as well as of estimated level splitting of 100 meV (given above). This means that free electrons with higher energies cannot be localized in the cluster, but could exist in extended states of the condensed sample.

These considerations indicate that, indeed, in the Debye mechanism only a countable number of electrons are participating. This is in accordance with the absence of the linear term of the specific heat of Au_{55} (section 5). However, it must be pointed out that the electronic states

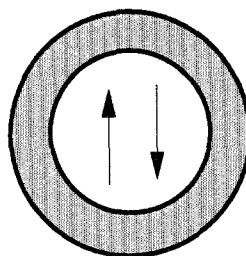


Fig. 11 The metal core of Au_{55} as a smallest quantum box containing two conductance electrons

participating in the mechanism must not all be “metallic” electrons in the cluster. Electronic states of the ligand shells can also contribute. The presence of reservoirs for electrons are favorable for potential SET processes. The inner shell(s) of the metal core may be effective wells and sinks [24]. This is supported by the finding via cyclic voltametry that an isolated Au_{55} cluster in solution can hold a number of additional electrons before it bursts [80].

The normalized high temperature conductivity for this process according to Eqs. (2), part II, approximately fits the SIMIT-data [24, 27, 81]. An explanation is given by the model in section 2.2, part II. In the high temperature range from 253 to 333 K – according to the fit – the capacitance C_{D} is not temperature dependent; hence, relation (4) implies that the microscopic Debye “conductivity process” seems to be thermally activated. However, for a purely “intra”-process this is quite improbable. Probably, the simple T^{-1} -dependence of the Debye process is proceeding in the interior of undisturbed densest packed regions of the sample (see also, section 2.2, part II). For the Cole–Cole hopping process which leads to percolation through the real sample across the constricted regions of the disturbed grain boundaries, a $T^{-1/2}$ -dependence is also possible, like that found for Au_{55} from 70 K and for Pd_{561} from 4.2 K up to their limit of thermal stability [72]. Already at the beginning of this section, it was pointed out that the occurrence of a CPE-element at the Cole–Cole process with an exponent $\alpha = 0.65$ can be interpreted as the consequence of a distribution of jump widths between neighboring clusters of a disturbed sample. Alternatively, such relaxation behavior can be explained by the existence of a distribution of activation enthalpies.

Because C_{D} remains constant, the assumption that practically all clusters of the undisturbed regions are participating in the Debye relaxation is favored by chemistry. It is plausible that in the high temperature region the clusters together with their ligand shell are rotating [82] or moving in such a way that the shells which include very different structure elements, are differently “opaque” at various places (see Fig. 1b for “normal” Au_{55}). By thermally induced motion and rotation they orientate themselves into

favorable positions for the electron transition. Freezing at lower temperatures would in fact increase the number of defects, making the undisturbed regions smaller. Finally, at low temperatures hopping-processes between neighboring clusters would predominate.

Optical properties of diluted and condensed ligand-stabilized metal cluster samples and miniband structure

In UV-visible absorption measurements in the range from 250 nm to 1350 nm, $\text{Au}_{55}(\text{PPh}_3)_{12}\text{Cl}_6$ dissolved in CH_2Cl_2 reveals a broad extended absorption over the whole frequency range without any fine structures. The spectrum is very similar to that of colloidal gold (15–20 nm in diameter) which has an already developed metallic band structure. This similarity indicates that the electronic level spacing within Au_{55} clusters must be quite small. The measured frequency range implies that if a band gap exists between valency and conduction band, it must be less than 1 eV. Solutions of Au colloid have a blood-red color due to the plasmon resonance (Mie-resonance) of the metallic particles, whereas solutions of Au_{55} clusters are brown-black (like the amorphous powders). This coloration does not give any hint of collective electronic behavior, as would be expected if the 6s-electrons were still completely delocalized. In the literature, the lack of plasma resonance is discussed with different proposals [55, 83]. The simplest explanation is that the particle size of Au_{55} is already too small to be sufficiently metallic.

Also, densest-packed samples of the normal Au_{55} cluster with a thickness up to 0.25 mm show a certain transparency for visible light in the range of 400 to 800 nm, although the samples are neither porous nor transparent by ocular observation [17, 18]. The interpretation used to explain the optical transparency of thin gold metal foils fails here because the Au_{55} samples are 100 times thicker than the gold foils. The Au_{55} pellets have a tarnished silver appearance like silicon or germanium. Thus, a similar explanation as that for red-transparent thin Si-layers could be applied here, assuming that a band structure with a band gap exists for the condensed ligand-stabilized cluster samples. Near the band gap the absorption process is not very intensive because such a process requires both a phonon and a photon.

To understand the behavior of the Au_{55} samples, one also has to take into account that the transparency can be switched by the same frequencies which are lying in the kHz- up to the MHz- range of the (Debye) relaxation modes (see section 6.1). For such an experiment the broad sides of the samples (approximately 20 mm²) were sputtered with gold layers of 10 nm thickness, yielding a good electrical contact, but only a weak absorption of the irra-

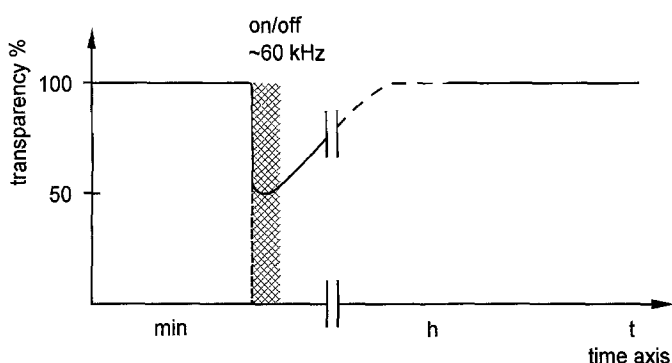


Fig. 12 Relative transparency of condensed material composed of "normal" Au_{55} . It can be switched by a Debye relaxation mode of about 60 kHz. This system returns only slowly back to its initial state

diated light. As diagrammed in Fig. 12, the transparency of the sample decreases to 50% of the original value as soon as the radio frequencies of the macroscopic resonance were applied. It is striking that above the resonance frequency and in the absence of an electrical field, the transparency does not increase immediately, but the system relaxes into the initial state after only a few hours.

The optical switching effect disappears, as is expected for the homogeneous dilution of the Au_{55} clusters in non-polar solid matrices like in polystyrene, which proves that this is most probably a collective effect. In samples with visible irregularities due to inefficient dispersion, e.g., cluster contents near 10%, this effect appears again as a result of cluster aggregation. Metal clusters in polar zeolitic matrices do not show this behavior due to the high dissolution.

To interpret the transparency and the switching behavior of the concentrated cluster samples, it may be tentatively assumed that the undisturbed regions with ideal cluster package have a band structure with a band gap in the order of magnitude of the energy of disproportionation of one cluster pair. The gap would be again in the same order as the level spacing within the cluster estimated before. The fine structures recognized in the differential conductivity by *Scanning Tunnel Spectroscopy (STS)* (~ 100 meV, see section 2.3, Fig. 11, part II) [28] and the calculated level spacing in the cluster (200–700 meV) [25] correspond to this value. Thus a picture arises of a perfect solid normally opaque to visible light, a novel semiconductor built up by a cluster collective. Its conduction "bands" would be nothing but extended states, which come into existence by the wave-mechanical coupling of neighboring states (c.f. section 2.5, Fig. 13, part II).

Regardless of whether these bands come into existence by many equal atom-orbitals (e.g., like the intrinsic bands of a semiconductor) discrete molecular-orbitals (genuine

minibands like for example at the condensed C_{60}) or as “hopping” bands [84], their band width will be different. Again, this width is dependent on the mutual influence of the cluster type in the packing. For the model system examined, for which a high symmetry was assumed, one can speak of “smallest bands” for single electrons. They originate from the overlapping of neighboring electron states which on their part are not existing in an isolated cluster. In a certain way these conduction bands are bands in “status nascendi,” which are occupied by the elementary step of the disproportionation of neighboring clusters and which, so to speak, are made use only for the transport. This band structure will also be overlapped by “hopping” bands from the unordered ranges. As a whole, at low temperatures, the dc-conductivity of compressed samples will be dominated by the latter [72]. Generally, one can expect that with increasing order the hopping bands will become genuine mini bands.

To understand why the samples darken during the application of the characteristic (Debye) macrofrequencies, key experiments are lacking especially at low temperatures. However, maintaining the picture of a novel solid with the smallest band structure, the loss of transparency can be explained by collective quantum properties. The electronic excitation of extended states could increase the concentration of delocalized electrons in a “diluted electron gas” thus “metallizing” the samples and decreasing the transparency. An explanation for the long “dead time” of the samples after turning off the external field could be the fact that the high order of the undisturbed regions hinders the “back reaction.” Another reason could be that the disturbed regions at the boundaries of the ideal grains inhibit percolation back to the initial state.

The above explanation offers a comparison with “porous silicium” which serves for the size-tailoring of electron wave-functions for the emission of light [10]. In this case, a “blue-shift” of the UV-excited VIS-emission with decreasing particle size has been shown. A further hint that electrons in their own, non-cluster “extended states” could be responsible for a wideband absorption is presented by the so-called “black sodalite” [49]. This sodalite is doped with Na-metal and absorbs in the visible range with increasing Na-surplus. The absorption is caused by electron transitions between neighboring Na_4^{3+} clusters. The increasing absorption by greater delocalization of the elections can also be observed visually by means of a color-change noted in the samples. Minor quantities of

Na color the sodalite “light blue” while increasing the Na concentration leads to transitions from “blue” to “purple” and finally to “black.” This color change seems to be caused by a matrix-bound metal-insulator-transition determined by the concentration of delocalized electrons which in turn is controlled by the synthesis. Until now, this transition could be observed by optical [49] and EPR-investigation [50], but not yet confirmed by electrical conductivity measurements. According to the Edwards–Sienko criterion [50], such a transition will be reached at a charge carrier concentration between 10^{27} and 10^{28} per m^3 . With the assumption that before electrical excitation, every cluster contributes merely one single electron to the dilute electron gas, the concentration is already $>10^{26}$ per m^3 . Thus, via the switching effect only a few additional electrons are necessary to surpass the critical charge carrier concentration in the diluted electron gas.

Due to a dilute electron gas constituted of mobile charges in extended states, the Au_{55} cluster samples are, in contrast, expected to be transparent according to the *Effective Medium Theory* (EMT) [85]. Because the similarity of compressed ligand-stabilized clusters with composite materials is currently being discussed, thus it is of interest to briefly mention the optical transparency of nanometal composite membranes [86] containing Au-metal particles which are colored due to the plasmon resonance. The transparency results from a reduced number of mobile charge (in comparison to metals). But the explanation for these Au-tubes in membranes cannot be used to describe the properties of compact Au_{55} (and other clusters) samples since they are much larger, with an inter-particle distance of approximately 50 nm.

Since this first part is immediately followed by part II. “Future directions,” a common outlook will be given at the end of the latter.

Acknowledgements We thank G. Schmid for cluster materials, intensive cooperation, stimulating discussions, and the exchange of newest ideas. We also thank U. Hartmann and R. Houbertz for their cooperation and unpublished measurements. We had helpful cooperation and many discussions on SET with A. Zorin. We gratefully acknowledge financial support by the Bundesminister für Forschung und Technologie (BMFT), Bonn, (Projekt Nr.: 03C 2005 8) under the coordination of the Deutsche Gesellschaft für das chemische Apparateswesen und Biotechnologie (DECHEMA), Frankfurt, and the latter for helpful discussions on particle-size effects.

References

- Ostwald W (ed) (1915) Die Welt der vernachlässigten Dimension, 1. Aufl, Th Steinkopff, Dresden
- Stauff J (1960) Kolloidchemie, Springer, Berlin-Göttingen-Heidelberg
- Henglein A (1987) Progr Colloid Polym Sci 73:1-4
- Brus LE (1983) J Chem Phys 79:5566; (1984) 80:4403; (1986) J Phys Chem 90:2555
- Henglein A (1992) Labor 2000 110
- Weller H (1993) Angew Chem 105:43-55
- Schmid G, Pfeil R, Boese R, Bandermann F, Mayer S, Calis GHM, van der Velden JWA (1981) Chem Ber 114:3634
- Mielke F, Houbertz R, Hartmann U, Simon U, Schön G, Schmid G (1994) Euro Phys Lett in press
- Pelster R, Marquardt P, Nimitz G, Enders A, Eifert H, Friedrich K, Petzold F (1992) Phys Rev B 46:8929-8933
- Ozin GA (1992) Adv Mater No 10 4:612-649
- Jacobs PA, Jaeger NI, Jiru P, Schulz-Ekloff G (eds) (1982) Metal Microstructures in Zeolites, Elsevier, Amsterdam
- Gügel A, Müllen K, Reichert H, Schmidt W, Schön G, Schüth F, Spikermann J, Titman J, Unger K (1993) Angew Chem No 4 105:618-619
- Grabert H, Devoret MH (eds) (1992) Single Charge Tunneling, Plenum, New York
- Gladun A, Zorin AB (1992) Phys i u Z No 4 23:159-165
- Licharev KK, Claesson T (1992) Spektr d Wiss 8:62-67
- Corcoran E (1992) Spektr d Wiss (Sonderheft 11) 1:76
- Schmid G, Schön G, Simon U (1992) German Patent pending No 42-12220
- Schmid G, Schön G, Simon U (1992) USA Patent pending No 08/041, 239
- Averin DV, Korotkov AN, Licharev KK (1991) Phys Rev B 44:6199
- Schmid G (1991) Mater Chem Phys 23:133
- Marquardt P, Börngen L, Nimitz G, Gleiter H, Sonnberger R, Zhu J (1986) Phys Letters 114 A:39
- Nimitz G, Marquardt P, Gleiter H (1988) J Crys Grow 86:66-71
- Marquardt P, Nimitz G (1989) Festkörperprobleme 29:317-328
- Simon U, Schön G, Schmid G (1993) Angew Chem Int Ed Engl No 2 32:250-254
- Häberlen OD, Chung S-C, Rösch N (1994) Ber Bunsenges Phys Chem No 6 98:882-885
- Gor'kov LP, Eliashberg GM (1965) Sov Phys JETP 21:940
- Simon U, Schmid G, Schön G (1992) Mat Res Soc Symp Proc Vol 272:167-175
- Hartmann U, Houbertz R, Mielke F, Simon U, Schön G, Schmid G (1995) to be published
- Schmid G, private communication
- Halperin WP (1986) Rev Mod Phys Vol 58 No 3:533-603
- Kimura K (1989) Z Phys D 11:327-332
- Averin AV, Licharev KK (1985) Proceedings of the Third International Conference on Superconducting Quantum Devices (SQUID's), Berlin, 197; (1986) J Low Temp Phys 62:345
- Licharev KK, Zorin AB (1985) J Low Temp Phys 59:347
- Fulton TA, Dolan GJ (1987) Phys Rev Lett 59:109
- Millikan RA (1909); see e.g. Wedler G (1982) Lehrbuch der Physikalischen Chemie, Verlag Chemie, Weinheim
- Fuchs K (1938) Proc Cambridge Phil Soc 34:100
- Schön G (1994) Spektr d Wiss 4:22-24
- Echt O, Sattler K, Recknagel E (1981) Phys Rev Lett 47:1127
- Ozin GA, Mitchell SA (1983) Angew Chem 95:706
- e.g. (1992) Ber Bunsenges Phys Chem No 9 96, Special Issue on Reactions in and with Clusters
- Cohen ML (1986) Proc 1st NEC Symp. Hakone and Kawasaki, Japan, p 2-10
- Schmid G (1992) Chem Rev 92:1709-1727; Schmid G (ed) (1994), VCH, Weinheim (Germany)
- Schmid G, Lehnert A, Malm J-O, Bovin J-O (1991) Angew Chem Int Ed Engl 30:852
- Ozin GA, Steele M (1992) Proc 9th Int Zeolite Assoc Conf, Montreal; Ozin GA, Özkaz S (1992) Chem Mater 4, 551
- Kawi S, Gates BC in Schmid G (ed) (1994), VCH, Weinheim (Germany)
- Breck DW (1974) Zeolite Molecular Sieves, John Wiley & Sons, New York
- Exner D, Jaeger NI, Kleine A, Schulz-Ekloff G (1988) J Chem Faraday Trans. 84(11):4097-4104
- Blatter F, Blazey KW (1990) IBM Research Report, Zürich
- Sradanov VI, Haug K, Metiu H, Stucky GD (1992) J Phys Chem 96:9039-9043
- Edwards PP, Woodall LJ, Anderson PA, Armstrong AR, Slaski M (1993) Chem Soc Rev 305-312
- Wang Y, Herron N, Mahler W, Suna A (1989) J Opt Soc Am B Vol 6 No 4:808-813
- Ozin GA, Kupermann A, Stein A (1989) Angew Chem Int Ed Engl 28:359
- Kappes M (1988) Chem Rev 86:1049
- Smit HHA, Nugteren PP, Thiel RC, de Jongh LJ (1988) Physica B 153:33
- Thiel RC, Benfield RE, Zanon R, Smit HHA, Dirken MW (1993) Struct Bond 81:2-35
- Smit HHA (1989) PhD Thesis Univ of Leiden, The Netherlands
- Goll G, Löhneysen HV, Kreibitz U, Schmid G (1991) Z Phys D 12:533
- Benfield RE, Creighton JA, Eadon DG, Schmid G (1989) Z Phys D 12:533
- Benfield RE, O'Brien P (unpublished work)
- de Jongh LJ, Brom HB, van Ruitenbeek JM, Thiel RC, Schmid G, Longoni G, Ceriotti A, Benfield RE, Zanon R, Pacchioni G, Bagus PS (ed) Cluster Models for Surface and Bulk Phenomena (NATO ASI Series B) Vol 283:151-168
- Fairbanks MC, Benfield RE, Newport RJ, Schmid G (1990) Sol St Comm 74:431
- Marcus MA, Andrews MP, Zegenhagen J, Bommannavar AS, Montano P (1990) Phys Rev B 42:3312
- Smit HHA, Thiel RC, de Jongh LJ, Schmid G, Klein N (1988) Sol St Com 65:915
- Wertheim GK, Di Cenzo SB, YOUNGQUIST SE (1983) Phys Rev Lett 51:2310
- Mason MG (1983) Phys Rev B 27:748
- Kittel C (1976) Festkörperphysik, John Wiley & Sons, New York
- de Jongh LJ, Baak J, Brom HB, van der Putten, van Ruitenbeek, Thiel RC (1992) Physics and Chemistry of Finite Systems: From Clusters to Crystals Vol 2:839-851
- Longoni G, Ceriotti A, Marchionna, Piro G (1988) Surface Organometallic Chemistry, Kluwer, The Netherlands
- Van Ruitenbeek JM, Jurgens MJGM, Schmid G, van Leeuwen DA, Zandbergen HW, de Jongh LJ (1990) Proc 5th Symp on Small Particles and Inorganic Clusters, Konstanz
- Wertheim GK (1990) Phase Transitions Vol 24-26:203-214
- Kubo R (1962) J Phys Soc Jpn 17:975
- van Staveren MPJ, Brom HB, de Jongh LJ (1991) Physics Reports 208:1-96
- e.g. Jonscher AK (1983) Dielectric Relaxation in Solids, Chelsea Dielectrics Press, London
- Macdonald JR (1987) Impedance Spectroscopy, John Wiley & Sons, New York
- Liedermann K, Loidl A (1993) J Non-Cryst Solids 155:26-36
- Simon U, Möhrke C (1993) Proc Meeting of the Dielectrics Society, Canterbury, UK
- Blümel R (1994) PhD Thesis University of Essen, Germany
- Zorin AB (1993) private communication
- Diot JL, Joseph J, Matin JR, Clechet P (1985) Electronanal Chem 199:75-88

80. Steggerda JJ, van der Linden JGM, Gootzen JEF (1992) Mat Res Soc Symp Proc Vol 272:127–132
81. Simon U (1992) PhD Thesis University of Essen, Germany
82. Schmid G (1993) private communication
83. Kreibig U, Fauth K, Granqvist C-G, Schmid G (1990) Z Phys Chem 169:11–28
84. Mott NF (1993) Conduction in Non-Crystalline Materials (2nd Ed), Clarendon Press, Oxford; and references therein
85. Aspens DE (1982) Thin Solid Films 89:249
86. Foss CA, Gabor L, Hornyak L, Stickert JA, Martin CR (1993) Adv Mater 5 No 2:135–136